2019 IEEE 30th Annual International Symposium on Personal, Indoor and Mobile Radio Communications (PIMRC): Track 1: Fundamentals and PHY

Ray Tracing Simulations in Millimeter-Wave Vehicular Communications

Bruno Colo, Abdurrahman Fouda and Ahmed S. Ibrahim
Department of Electrical and vehicle Engineering
Florida International University, Miami, Florida, USA 33174
Emails: {bcolo015, afoud004, aibrahim}@fiu.edu

***Abstract*—Autonomous vehicles are equipped with multiple high-resolution sensors and cameras for an accurate local view of their surroundings. Equally important, they will need to exchange such high data-rate among each other for a wider view of their environments. The use of high-bandwidth millimeter-wave (mmWave) spectrum bands in vehicular communications can satisfy such demand for high data-rate exchange. Before attempting to design any mmWave vehicular communication system, there is a need to fully understand the propagation characteristics of such mmWave mobile environment. In this paper, we leverage the ray tracing capabilities in the WinProp software suite and study the propagation characteristics of mmWave channels in vehicular communications. In doing so, we present the implementation of the Vehicle-to-Infrastructure (V2I) communication scenario in WinProp. Via simulation results, we are able to show that approximately 20 dB degradation of signal strength can happen within 5 seconds.**

***Index Terms*—millimeter-wave, ray tracing, vehicle-to-infrastructure, vehicular communication, WinProp.**

I. Introduction

There is a huge interest in developing autonomous vehicles, or self-driving vehicles [1]. Such vehicles will rely on a large number of various high-resolution cameras and sensors. For example, LIght Detection And Ranging (LIDAR) technology can be utilized for 3-dimensional (3D) mapping [2] for accurate target detection and velocity estimation. However, these sensors will only provide a local view of the surrounding environment. For a wider view, autonomous vehicles will need to communicate with each other, i.e., Vehicle-to-Vehicle (V2V), as well as with the surrounding infrastructure, i.e., Vehicle-to-Infrastructure (V2I).

The transmission of these collected measurements among vehicles and Road Side Units (RSUs) will require high data rate, in the order of hundreds of Kbps to hundreds of Mbps [3]. For example, LIDAR requires data rate in the $10-100\,\mathrm{Mbps}$ range. This cannot be supported via the current vehicle-specific dedicated short-range communication (DSRC) protocol given its limited data rate of $6\,\mathrm{Mbps}$ [3]. Given the need to exchange the data captured by sensors and cameras, which are high-data-rate information, we aim to utilize the high-bandwidth millimeter-wave (mmWave) spectrum band. Due to their potential high-bandwidth, they can carry a huge amount of information among vehicles and RSUs.

The challenges in fixed mmWave communications have been studied [4], [5] and they include low-range and low-penetration through surfaces [6]. Typically, having the receiver and transmitter within close proximity as well as having a direct line of sight between the both of them are essential requirements [7], [8]. Vehicular communication over mmWave band [3], [9] has received recent attention including the works on analyzing the coherence time to choose the optimal beamforming beamwidth and beam realignment [10], [11]. However, there has been no investigation aiming to understand the behavior of the mmWave channels in vehicular environments. Therefore, providing accurate characterization of the mmWave propagation characteristics in vehicular communication is the scope of this paper.

In this paper, we consider the ray tracing approach, as a reliable methodology, to estimate the propagation characteristics. Ray tracing approach is highly efficient in capturing the effects of the waves' reflections on buildings, and the irregularities present on such buildings [12]. In particular, we utilize the WinProp software suite, which implements a ray tracing approach, to analyze the vehicular environment in the mmWave spectrum band. We focus on the V2I communication scenario allowing one transmitting vehicle to move in an urban environment, while the receiving RSU is fixed at a specific location. In such deployment model, we can investigate the quality of the mmWave vehicular communication in both line-of-sight (LoS) and non-light-of-sight (NLoS) conditions.

The rest of this paper is organized as follows. In Section II, we introduce the simulation methodology describing the simulation environment and vehicle trajectory. Section III presents the simulation results illustrating the behavior of vehicular communication in mmWave spectrum band. Finally, Section IV presents the conclusion and future works.

This work is supported in part by the National Science Foundation under Award No. CNS-1816112.

978-1-5386-8110-7/19/$31.00 ©2019 IEEE

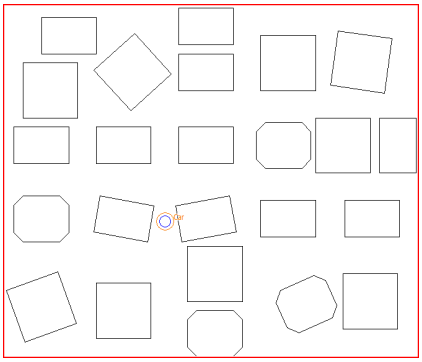

Fig. 1: Urban simulation environment with buildings of different sizes and shapes. The initial position of the moving vehicle is illustrated.

II. Simulation Methodology

In this section, we describe the simulation methodology, which consists of developing the simulation environment along with deploying a vehicle transmitting site and creating its trajectory. We have designed a simulation map (database) to mimic an urban environment. As shown in Fig. 1, it consists of several buildings of different areas, heights, and materials. All these details were specified using WallMan, which is one of the programs included in the WinProp suite.

The simulation map was then imported into ProMan, which is the software that renders the actual coverage map. The x coordinate for the simulation area varies from $-110\,\mathrm{m}$ to $117\,\mathrm{m}$, and the y coordinate goes from $-90\,\mathrm{m}$ to $102\,\mathrm{m}$, making this database measure $227\,\mathrm{m} \times 192\,\mathrm{m}$, for a total of $43,584\,\mathrm{m}^2$. Fig. 1 also shows the initial position $(-22\,\mathrm{m}, -16\,\mathrm{m})$ of the movable transmitter site "vehicle". A single omni-directional antenna, at a height of $1.5\,\mathrm{m}$, is installed at the vehicle's roof. An omni-directional antenna propagation model was considered to satisfy the need for vehicles to symmetrically communicate in all directions. The mmWave transmission frequency is equal to 30 GHz, and the total transmission power is equal to 5 watts. Finally, the speed of the vehicle is set to $20\,\mathrm{m/s}$, equivalent to approximately $45\,\mathrm{mph}$. As for the vehicle's trajectory, it will initially move north for $3.1\,\mathrm{s}\,(62\,\mathrm{m})$, reaching coordinate $(-22\,\mathrm{m}, 46\,\mathrm{m})$. Then, it makes a right turn and moves east for $2.9\,\mathrm{s}\,(58\,\mathrm{m})$, ending in coordinate $(36\,\mathrm{m}, 46\,\mathrm{m})$, having then moved for a total of $6\,\mathrm{s}\,(120\,\mathrm{m})$.

Our goal is to investigate the coverage map as the vehicle travels in its trajectory. In doing so, we create a sequence of snapshots that are separated by $100\,\mathrm{ms}\,(2\,\mathrm{m})$. Such process results in a total of 61 snapshots, from $t_{\mathrm{init.}} = 0.0\,\mathrm{s}$ to $t_{\mathrm{fin.}} = 6.0\,\mathrm{s}$. In each snapshot (time stamp), WinProp provides the signal-to-interference-plus-noise ratio (SINR) map of all positions within the area of consideration. Given these data sets, we can analyze the impact of the vehicles movement on the SINR coverage at a specific position. In other words, it becomes possible to see how the vehicle's position affects the strength of the received signal at a particular RSU location. We will, in the following section, choose three points to be analyzed further.

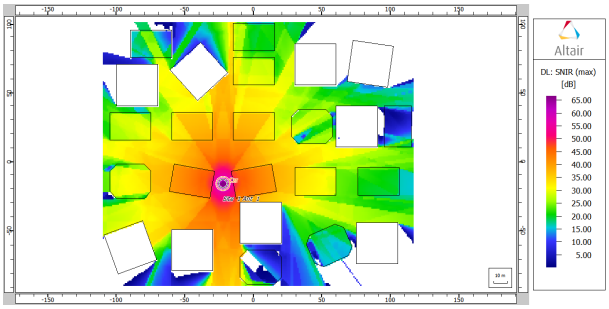

Fig. 2: SINR coverage map for the initial position ($t = 0.0\,\mathrm{s}$).

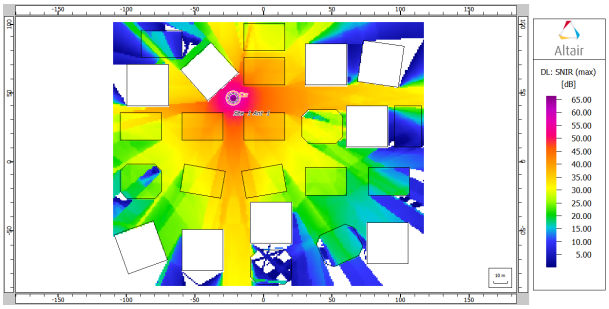

Fig. 3: SINR coverage map for the middle position ($t = 3.1\,\mathrm{s}$).

III. Simulation Results

In this section, we study the impact of the transmitted mmWave signal from the mobile vehicle on the coverage map of the urban environment under consideration. First, Figs. 2-4 show the change in the SINR map while the vehicle is in the beginning, middle, and end of the trajectory, respectively. As expected, the center of the high-SINR region moves along with the vehicle. In addition to showing coverage gaps, we can analyze specific locations for the RSU in terms of its received SINR throughout the whole travel time. For instance, we consider point $\mathrm{P}_1 = (-66.5\,\mathrm{m}, -6.5\,\mathrm{m})$ for the RSU, which is shown as a square in Fig. 5, along with the vehicle's trajectory.

Fig. 6 depicts the received SINR at point P_1, as the vehicle travels through its trajectory. As shown in Fig. 6, first there is a sharp increase in the SINR between time intervals $t = 0.6\,s$ and $t = 1.4\,s$. Such rapid change is a result of having an LoS condition between the vehicle and the RSU, located at position P_1. The decrease of signal strength thereafter is an indication that the vehicle is getting further away from the potential RSU location and is becoming in an NLoS condition with the RSU. We point out that large SINR degradation of about 20

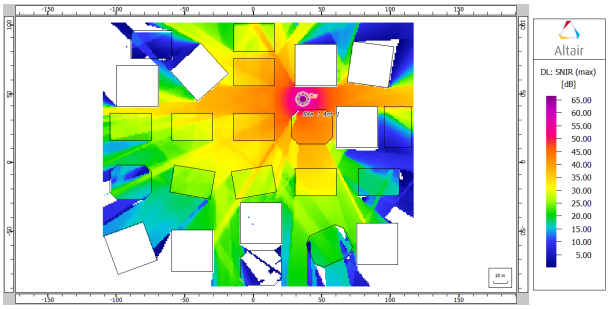

Fig. 4: SINR coverage map for the last position ($t = 6.0s$).

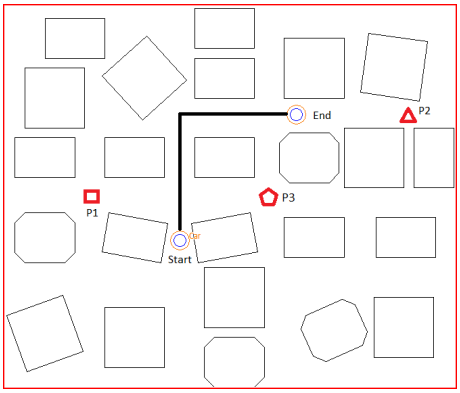

Fig. 5: vehicle trajectory along with three points of interest.

dB happens within $5\,\mathrm{s}$, which will be very challenging for any mmWave vehicular communication system.

Similarly, we can consider point $\mathrm{P}_2 = (92.5\,\mathrm{m}, 46.5\,\mathrm{m})$, shown in Fig. 5 as a triangle, as a potential position for the RSU. In this case and as opposed to the P_1 location, the vehicle will be moving closer to the RSU. Fig. 6 shows the received SINR at the potential RSU location as the vehicle moves in its trajectory. As shown, the SINR increases gradually until direct LoS is achieved, indicated by the sudden jump in SINR between time stamps $t = 2.2\,\mathrm{s}$ and $t = 2.6\,\mathrm{s}$. It then grows linearly as the vehicle moves towards the P_2 RSU location. The last RSU location is point $\mathrm{P}_3 = (24.5\,\mathrm{m}, 6.5\,\mathrm{m})$, shown in Fig. 5 as a pentagon. In this final case, LoS is achieved briefly, at the same time as P_1. This results in both points P_1 and P_3 having similar SINR curves, initially. However, as the vehicle continues its trajectory, LoS is achieved again once more in P_3, whereas it does not in P_1. This means the SINR for P_3 will drastically rise again, as expected for a gain of LoS. This may be seen to happen between time stamps $t = 4.9\,\mathrm{s}$ and $t = 5.6\,\mathrm{s}$. LoS conditions are also shown in Fig. 7 for all three of the mentioned RSU locations.

Lastly, Fig. 8 depicts the dependency of the SINR with the distance of the V2I communication. In other words, instead of relating the SINR received at each point with

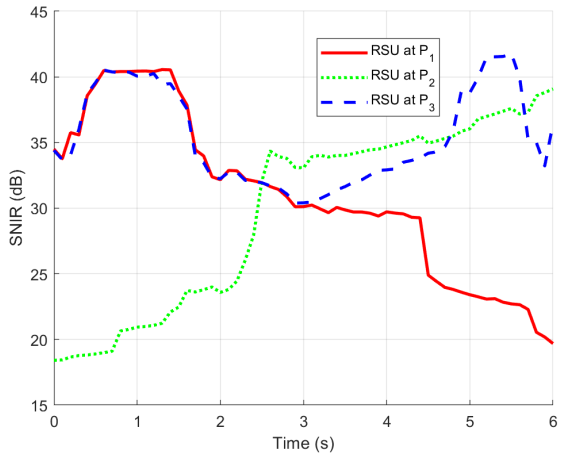

Fig. 6: Received SINR values at RSU locations P_1, P_2 and P_3 with respect to time.

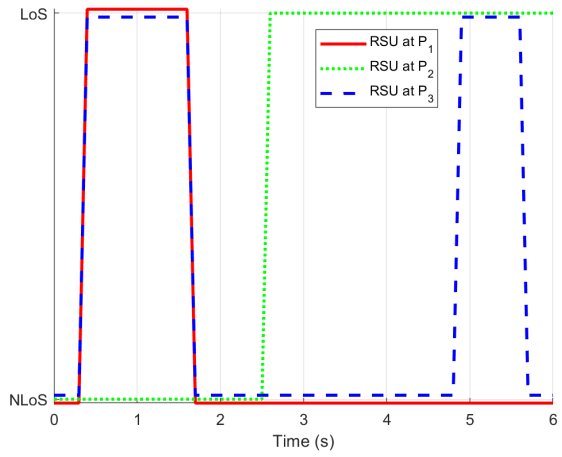

Fig. 7: LoS condition at RSU locations P_1, P_2 and P_3.

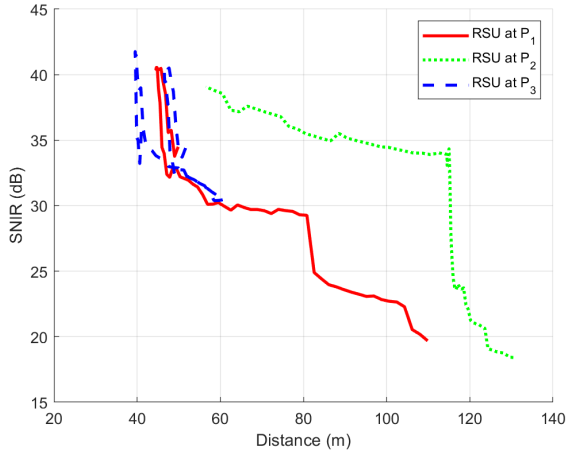

Fig. 8: Received SINR values at RSU locations P_1, P_2 and P_3 with respect to distance.

time, we may instead relate it with the distance between the given point and the vehicle's position at that instance of time. In Fig. 8, we observe that the curves for points P_1 and P_2 share curves with a similar shape. This may be justified as they share similar behaviors. In P_1's case, the vehicle momentarily has a LoS condition to the point and loses it as the vehicle moves further away without regaining LoS again. In P_2's case, the reverse behavior is observed, where the vehicle comes closer to P_2 in NLoS condition until it is reached for the remainder of the path. Point P_3 deviates from this curve aspect as the LoS condition is achieved twice and the variation in distance is much lower than in the previous two cases. We also see that curves from points P_1 and P_3 practically overlap momentarily. This is consistent with the previous result shown in Fig. 6.

IV. Conclusion

This paper is considered as a first step in understanding the propagation challenges in mmWave vehicular communications. We have shown that sharp decrease of $20\,\mathrm{dB}$ in the SINR can happen within $5\,\mathrm{sec}$, which will be very challenging for the design of any vehicular communication system. We will continue this work by considering multiple extensions. First, we will investigate the impact of doppler spread. Second, we will deploy multiple vehicles that are communicating at the same time, which will lead to interference.

References

[1] F. Rossi, R. Zhang, Y. Hindy, and M. Pavone, "Routing autonomous vehicles in congested transportation networks: Structural properties and coordination algorithms," *Auton. Robots*, vol. 42, no. 7, pp. 1427–1442, Oct. 2018.

[2] J. Li, H. Bao, X. Han, F. Pan, W. Pan, F. Zhang, and D. Wang, "Real-time self-driving car navigation and obstacle avoidance using mobile 3D laser scanner and GNSS," *Multimedia Tools Appl.*, vol. 76, no. 21, pp. 23 017–23 039, Nov. 2017.

[3] J. Choi, V. Va, N. Gonzalez-Prelcic, R. Daniels, C. R. Bhat, and R. W. Heath, "Millimeter-Wave vehicular communication to support massive automotive sensing," *IEEE Commun. Mag.*, vol. 54, no. 12, pp. 160–167, December 2016.

[4] T. S. Rappaport, S. Sun, R. Mayzus, H. Zhao, Y. Azar, K. Wang, G. N. Wong, J. K. Schulz, M. Samimi, and F. Gutierrez, "Millimeter wave mobile communications for 5G cellular: It will work!" *IEEE Access*, vol. 1, pp. 335–349, 2013.

[5] S. Huang, Y. Gao, W. Xu, Y. Gao, and Z. Feng, "Energy-angle domain initial access and beam tracking in Millimeter Wave V2X communications," *IEEE Access*, vol. 7, pp. 9340–9350, 2019.

[6] A. Perez, A. Fouda, and A. S. Ibrahim, "Ray tracing analysis for UAV-assisted integrated access and backhaul millimeter wave networks," in *Proc. IEEE WoWMoM Workshop Wireless Netw. Planning Comput. UAV Swarms*, Washington, DC, USA, Jun. 2019.

[7] M. A. Abdel-Malek, A. S. Ibrahim, and M. Mokhtar, "Optimum UAV positioning for better coverage-connectivity tradeoff," in *Proc. IEEE 28th Annu. Int. Symp. on Pers., Indoor, Mobile Radio Commun. (PIMRC)*, Oct 2017, pp. 1–5.

[8] M. A. Abdel-Malek, A. S. Ibrahim, M. Mokhtar, and K. Akkaya, "UAV positioning for out-of-band integrated access and backhaul millimeter wave network," *Phys. Commun.*, vol. 35, p. 100721, Aug. 2019.

[9] T. Rappaport, R. Heath, R. Daniels, and J. Murdock, *Millimeter Wave wireless communications*. Prentice Hall, 2015.

[10] V. Va and R. W. Heath, "Basic relationship between channel coherence time and beamwidth in vehicular channels," in *Proc. IEEE Vehic. Technol.Conf. (VTC)*, Sep. 2015, pp. 1–5.

[11] V. Va, J. Choi, and R. W. Heath, "The impact of beamwidth on temporal channel variation in vehicular channels and its implications," *IEEE Trans. Veh. Technol.*, vol. 66, no. 6, pp. 5014–5029, June 2017.

[12] E. M. Vitucci, J. Chen, V. Degli-Esposti, J. S. Lu, H. L. Bertoni, and X. Yin, "Analyzing radio scattering caused by various building elements using Millimeter-Wave scale model measurements and ray tracing," *IEEE Trans. Antennas Propag.*, vol. 67, no. 1, pp. 665–669, Jan 2019.